

# Measuring liver T2\* and cardiac T2\* in a single acquisition

Suraj D. Serai,<sup>1,2</sup> Andrew T. Trout,<sup>1</sup> Robert J. Fleck,<sup>1</sup> Charles T. Quinn,<sup>3</sup>  
Jonathan R. Dillman<sup>1</sup>

<sup>1</sup>Department of Radiology, MLC 5031, Cincinnati Children's Hospital Medical Center, 3333 Burnet Avenue, Cincinnati, OH 45229, USA

<sup>2</sup>Department of Radiology, Children's Hospital of Philadelphia, 3401 Civic Center Blvd, Philadelphia, PA 19104, USA

<sup>3</sup>Department of Hematology, Cincinnati Children's Hospital Medical Center, 3333 Burnet Avenue, Cincinnati, OH 45229, USA

## Abstract

**Purpose:** The purpose of this study is determine if both liver T2\* and cardiac T2\* can be measured on a single breath-hold acquisition.

**Materials and methods:** For this IRB-approved retrospective study, 137 patients with dedicated Cardiac MRI and Liver MRI examinations obtained sequentially on 1.5T scanners and on the same day were included for analysis. Both the cardiac and liver MRI examinations utilized GRE sequences for quantification of tissue iron. Specifically, T2\* was measured using an 8-echo, multi-echo gradient echo single breath-hold sequence. Liver T2\* was measured in a blinded manner on images from each of the cardiac and dedicated liver MRI examinations and were correlated. Bland–Altman difference plot was used to assess mean bias.

**Results:** 137 examinations from 93 subjects met inclusion criteria. 10 examination pairs were excluded because the first echo time (TE) on the cardiac MRI was insufficiently short for the very high liver iron content. After exclusion, 127 studies from 89 subjects (67.4% males) were included in the final analysis. The mean subject age ( $\pm$  standard deviation) was  $11.5 \pm 7.5$  years (range 0–29.3 years; median 10.5 years). Mean liver T2\* measured on cardiac MRI was  $8.3 \pm 7.7$  ms and mean liver T2\* measured on dedicated liver MRI was  $7.8 \pm 7.4$  ms ( $p < 0.001$ ). There was strong positive correlation between the two liver T2\* measurements ( $r = 0.989$ ,  $p < 0.0001$ ; 95% CI 0.985–0.992). With the exception of borderline outliers, all values fell within two standard deviations on the Bland–Altman difference plots, with a mean bias of 0.5 ms (range  $-1.8$  to  $+2.7$  ms).

**Conclusion:** In most patients with suspected or known iron overload, a single breath-hold GRE sequence may be sufficient to evaluate the iron concentration (T2\*) of both the myocardium and the liver.

**Key words:** Liver iron—Cardiac iron—Liver R2\*—T2\*—Cardiac T2\*

Iron deposition in the liver can be the result of multiple transfusions of red blood cells given for chronic or recurrent anemia, hereditary or acquired states of ineffective erythropoiesis (e.g., non-transfusion-dependent thalassemia or myelodysplastic syndrome), or genetic hemochromatosis, in which there is abnormally increased intestinal absorption of iron. Iron overload in the liver has been associated with liver injury and dysfunction, including fibrosis, cirrhosis, and hepatocellular carcinoma (HCC) [1, 2]. The diagnosis of hepatic iron deposition and quantification of liver iron burden traditionally relied on core liver biopsy, which is limited by invasiveness, sampling error, and subjectivity in interpretation [3]. In the current era, MRI has largely taken over as the diagnostic modality of choice for the identification and quantitation of hepatic iron deposition [4–6]. MRI has been shown to accurately quantify the liver iron content without the need for invasive biopsy, thereby allowing regular, serial assessments that can guide chelation therapy or therapeutic phlebotomy [7].

One MRI technique that is used for liver iron content (LIC) quantification is a T2\*-based gradient echo multi-echo image acquisition in which a series of images are obtained with increasing echo times (TE) to generate a T2\* decay curve [5, 8]. The signal decay rate is then calculated based on an exponential fit to the generated

curve and is expressed in terms of ms (T2\*) or 1/s (R2\*) [4, 5, 9, 10]. Liver signal decay values thus obtained can be converted to LIC which has been shown to be a reasonable surrogate for total body iron stores [5, 8, 11]. While LIC is reflective of total body iron stores, it has limited predictive value for other end-organ (pancreas, heart, etc.) involvement by disease [10]. Therefore, to monitor iron levels in the liver and the heart, dedicated imaging of each organ is generally required. At our institution, this is achieved with separate MRI examinations of the liver and heart. However, the multi-echo gradient echo sequence utilized for quantification of myocardial iron generally includes the liver in the field of view, and, thus, there is a potential to quantify both myocardial and hepatic iron contents in a single imaging sequence, potentially saving scanner and patients' time and reducing healthcare cost.

In this retrospective study, we aimed to define the feasibility and accuracy of a single breath-hold GRE-based sequence to compute both myocardial and hepatic iron contents. We also examined the relationship of liver T2\* values to pancreas (included in the field of view) T2\* values and of pancreas T2\* to cardiac T2\* in the same patient.

## Materials and methods

This retrospective study was IRB-approved, and all study procedures were performed in a HIPAA-compliant manner. Our Department of Radiology PACS system (Merge; Chicago, IL, USA) searched for all patients who had a dedicated cardiac MRI examination for evaluation of cardiac T2\* and a liver MRI examination for evaluation of liver T2\* on the same day and on the same MRI scanner between May 1, 2010 and January 31, 2017.

All MRI examinations were acquired at 1.5T MR field strength utilizing either a GE MR scanner (Model: HDx, GE Healthcare, Waukesha, USA) equipped with a gradient system with a maximum amplitude of 33 mT/m and a 150 mT/m/ms slew rate using the 8-channel Cardiac-Torso coil or a Philips MR scanner (Model: Ingenia, Philips Healthcare, Best, The Netherlands) equipped with a gradient system with a maximum amplitude of 45 mT/m and a 200 mT/m/ms slew rate using the anterior-posterior Torso coil combination. For both the cardiac and liver examinations, T2\* images for LIC calculation were acquired using an 8-echo, multi-echo gradient echo single breath-hold sequence lasting approximately 12–15 s as described previously and as detailed in Table 1 [5, 6, 12, 13]. Of note, the minimum TE utilized for the dedicated cardiac MRI examinations was longer than the minimum TE for the dedicated liver exams due to the oblique (cardiac short-axis) plane of acquisition. Patients were excluded from our analyses if liver iron levels were so high that the first TE was insufficiently short and resulted in a lack of hepatic signal on the cardiac MRI images.

**Table 1.** Pulse sequence parameters for T2\* sequence used for liver MRI and cardiac MRI

Sequence	T2* liver MRI	T2* cardiac MRI
Scan mode	2D	2D
TR (ms)	7.1	18
No. of echoes	8	8
First TE (ms)	0.9	2.1
Delta TE (ms)	0.8	2.1
Flip angle	25	20
Matrix size	140 × 140	196 × 124
Slice thickness (mm)	6	6
Acceleration factor	1.5	1.5
No. of slices	6	3
Scan time (s)	0:10	0:15

TE, echo time; TR, repetition time; msec, time in milliseconds

For both the liver and cardiac MRI examinations, liver T2\* maps were generated using a commercially available curve fitting software, MEDIS (Medis Medical Imaging Systems, Leiden, The Netherlands), and T2\* measurements were performed by a single trained observer who drew regions of interest (ROI) that encompassed as much of the liver as possible while avoiding large vascular structures on four axial images through the mid liver; as previously described [5]. ROI size varied within and between patients based on liver size, orientation, and position of large vascular structures. T2\* values in each patient were calculated as the mean of the four individual T2\* measurements. Liver T2\* measurements made from dedicated liver and cardiac MRI examinations were obtained in a blinded manner. Single exponential fitting was utilized for T2\* decay curve fitting and, for cases of rapid signal decay (high levels of iron), the software allows for truncation of the data to exclude later echoes that consist essentially of noise. Using liver T2\*, LIC values were calculated from the formula as described by Wood et al. [11]. Pancreas T2\* measurements were also obtained in a similar manner from dedicated liver MR images, with a single ROI placed in the body of the pancreas. Cardiac myocardial T2\* values were also measured on dedicated short-axis cardiac images by placing a single ROI on the mid-myocardium slice.

## Statistical analyses

Statistical analyses were performed using MedCalc (MedCalc, Ostend, Belgium). Pearson correlation was used to assess the relationship of liver T2\* measurements obtained using dedicated liver MRI versus cardiac MRI. Paired t-tests (2-tailed) were done to compare the means. Scatter plots and Bland-Altman difference plots also were generated to assess the agreement between the two methods. 95% confidence and prediction limits were added to identify and display outliers. A sub-analysis was performed on patients with substantially high liver iron

( $T2^* < 5$  ms) to validate if the same correlation relationship also existed in this subpopulation. Pancreas T2\* values were correlated (Pearson) with liver and cardiac T2\* to test the hypothesis that pancreas T2\* values correlate with, and are predictive of, cardiac iron loading.

## Results

137 pairs of liver and cardiac T2\* examinations from 93 subjects were identified. 10 examination pairs in 4 patients were excluded because the first TE in the dedicated cardiac exam was insufficiently short for the high degree of liver iron overload. Among the final study population of 89 patients with 127 cardiac and liver MRI examinations pairs, 57.4% (73/127) were male with a mean age ( $\pm$  standard deviation) of  $11.5 \pm 7.5$  years (range 0–29.3 years; median 10.5 years). Indications for iron quantification included beta thalassemia ( $n = 42$ , 33.1%), Diamond–Blackfan anemia ( $n = 42$ ), prior marrow transplant ( $n = 12$ ), sickle cell disease ( $n = 8$ ), other transfusion-dependent anemia ( $n = 7$ ), Glanzmann’s thrombasthenia ( $n = 2$ ), dyskeratosis congenita ( $n = 2$ ), prior liver transplant ( $n = 2$ ), congenital neutropenia ( $n = 2$ ), acute lymphoblastic leukemia ( $n = 1$ ), portal vein thrombosis ( $n = 1$ ), short gut ( $n = 1$ ), prior multi-visceral transplant ( $n = 1$ ), neonatal liver failure ( $n = 1$ ), sideroblastic anemia ( $n = 1$ ), Fanconi anemia ( $n = 1$ ), and history of peripheral neuroendocrine cell tumor ( $n = 1$ ).

Mean liver T2\* measured on the cardiac MRI examinations was  $8.3 \pm 7.7$  ms compared with  $7.8 \pm 7.4$  ms on the dedicated liver MRI examinations ( $p < 0.001$ ). Mean calculated LIC from the dedicated liver MRI examinations was 12.7 mg/g (range 4.0–37.4). Measured liver T2\* was strongly and positively correlated between the two examinations,  $r = 0.989$  ( $p < 0.0001$ ; 95% CI 0.985–0.992, Fig. 1). Based on Bland–Altman analysis, the mean bias in measured T2\* between sequences was + 0.5 ms (range – 1.8 to + 2.7) (Fig. 2). Six measurement pairs fell on or just outside the 95% confidence limits for the line of best fit and fell outside of two standard deviations from the mean on Bland–Altman analysis. Four of the six outliers had mean T2\* > 20 ms (a normal result), and two outliers had mean T2\* between 10 and 20 ms.

70 examination pairs (55.1%) had a liver T2\* less than 5 ms by both techniques. For this sub-group, there was moderate to strong correlation between T2\* measurements obtained on dedicated liver versus cardiac imaging ( $r = 0.79$ ;  $p < 0.0001$ ; 95% CI 0.69–0.86). Four measurement pairs fell on or just outside the 95% prediction limits for the line of best fit (Fig. 3A). Based on Bland–Altman analysis, the mean bias in measured liver T2\* between the dedicated cardiac and liver examinations (C-Liver T2\*–L-Liver T2\*) was + 0.41 ms (range – 0.82 to

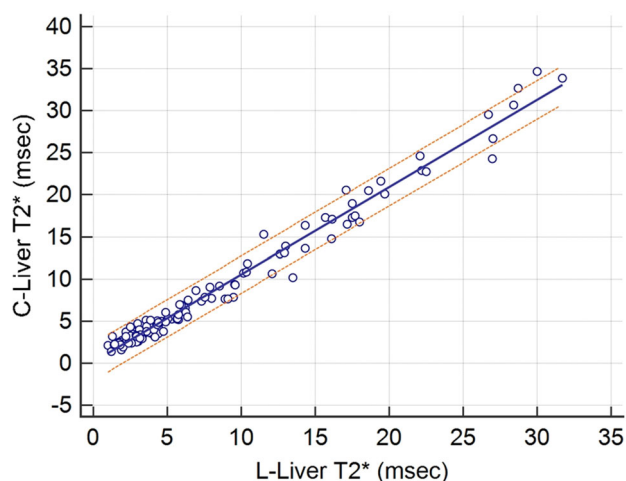


Fig. 1. Scatterplot of liver T2\* values obtained on the dedicated cardiac MRI study (y-axis) vs. liver T2\* values obtained on the dedicated liver MRI study ( $n = 127$ ;  $r = 0.98$ ; 95% CI 0.98–0.99;  $p < 0.0001$ ). Solid blue line is the line of best fit with the dotted red lines representing the 95% prediction limits for the best fit line.

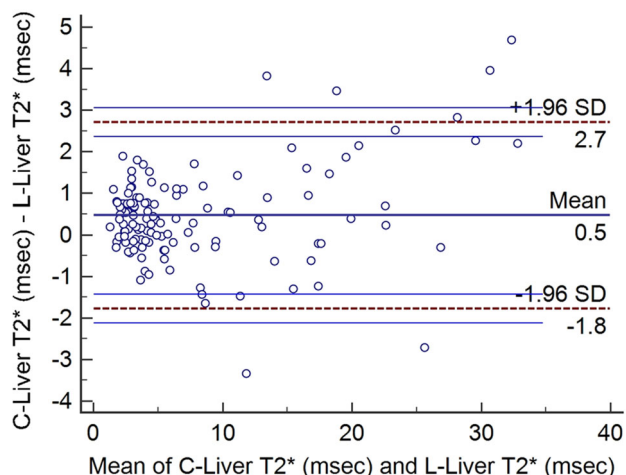
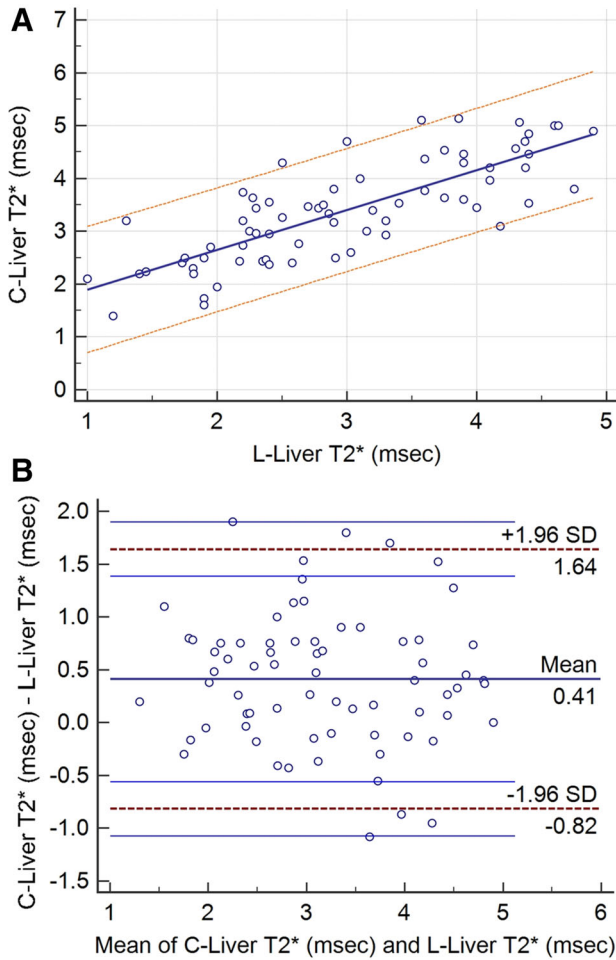


Fig. 2. Bland–Altman difference plot of liver T2\* values obtained on the dedicated cardiac MRI study vs. liver T2\* values obtained on the dedicated liver MRI study showing all values falling within two standard deviations, with a mean bias of only 0.5 ms ( $\pm 1.96$  SD: – 1.8 to + 2.7 ms) with the exception of 6 borderline outliers. Dotted red lines demarcate 1.96 standard deviations of the mean difference and thin solid blue lines demarcate the 95% prediction limits of the standard deviations.

+ 1.64) with all values falling within two standard deviations of the mean (Fig. 3B).

For all 127 examination pairs included in the study, there were weak correlations between pancreas and liver T2\*,  $r = 0.49$  ( $p < 0.0001$ ; 95% CI 0.35–0.62) (Fig. 4); liver and cardiac T2\*,  $r = 0.32$  ( $p = 0.0002$ ; 95% CI



**Fig. 3. A** For patients with substantially high liver iron ( $T2^* < 5$  ms), a scatterplot of liver  $T2^*$  values obtained on the dedicated Cardiac MRI study ( $y$ -axis) vs. liver  $T2^*$  values obtained on the dedicated Liver MRI study ( $x$ -axis) showing a correlation coefficient,  $r = 0.79$  (95% CI 0.69–0.86;  $n = 70$ ,  $p < 0.0001$ ). Solid blue line is the line of best fit with the dotted red lines representing the 95% prediction limits for the best fit line. **B** On the same patient population, Bland–Altman difference plot of liver  $T2^*$  values obtained on the dedicated Cardiac MRI study vs. Liver  $T2^*$  values obtained on the dedicated Liver MRI study showing a mean bias of only 0.41 ms ( $\pm 1.96$  SD:  $-0.82$  to  $+1.64$ ). Dotted red lines demarcate 1.96 standard deviations of the mean difference and thin solid blue lines demarcate the 95% prediction limits of the standard deviations.

0.15–0.47) (Fig. 5); and pancreas and cardiac  $T2^*$ ,  $r = 0.27$  ( $p = 0.0019$ ; 95% CI 0.10–0.43) (Fig. 6).

## Discussion

The treatment of iron overload depends on its cause, severity, duration, and organ distribution. The primary treatment for tissue iron overload due to multiple or chronic transfusions is chelation therapy, which is titrated to maintain sufficiently low total body iron stores

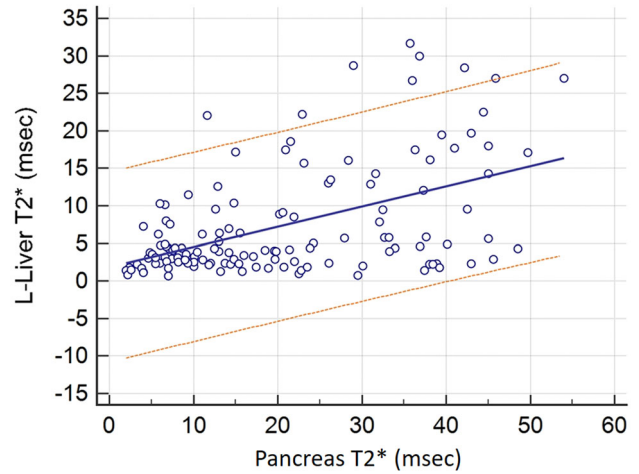


**Fig. 4.** Scatterplot of liver  $T2^*$  values obtained on the dedicated liver MRI study ( $y$ -axis) vs. pancreas  $T2^*$  values obtained on the dedicated Liver MRI study ( $x$ -axis) ( $n = 127$ ;  $r = 0.49$ ; 95% CI 0.35–0.62;  $p < 0.0001$ ). Solid blue line is the line of best fit with the dotted red lines representing the 95% prediction limits for the best fit line.

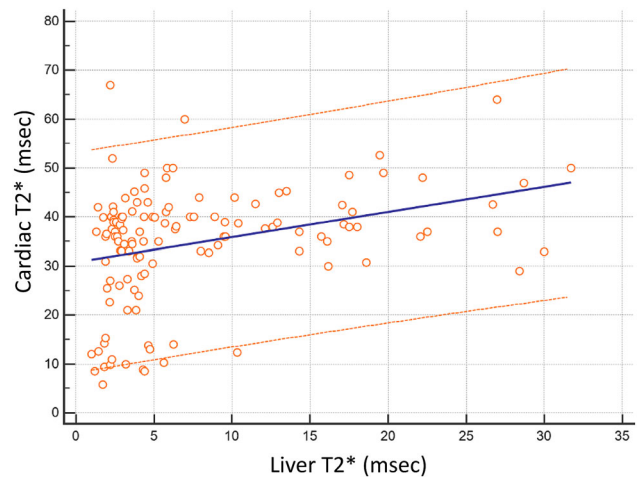


**Fig. 5.** Scatterplot of cardiac  $T2^*$  values obtained on the dedicated cardiac MRI study ( $y$ -axis) vs. liver  $T2^*$  values obtained on the dedicated liver MRI study ( $x$ -axis) ( $n = 127$ ;  $r = 0.32$ ; 95% CI 0.15–0.47;  $p = 0.0002$ ). Solid blue line is the line of best fit with the dotted red lines representing the 95% prediction limits for the best fit line.

to prevent iron toxicity while minimizing treatment side effects. To achieve this, accurate quantification of tissue iron content is necessary. MRI relaxometry-based  $T2^*$  measurements have been established as a repeatable and reproducible measure of LIC [4, 5, 8–10, 14]. Because LIC is not a perfect marker for the state of disease and iron loading and iron clearance rate may be organ-dependent [15], dedicated imaging of the heart for myocardial iron quantification is required in patients at high risk of cardiac iron deposition. This typically re-

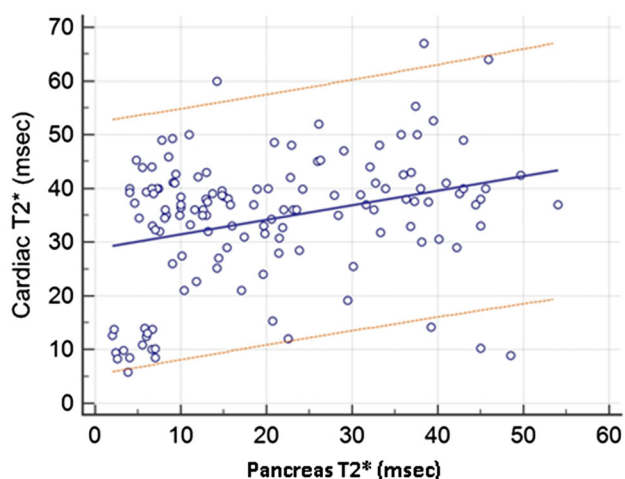


**Fig. 6.** Scatterplot of cardiac T2\* values obtained on the dedicated cardiac MRI study (y-axis) vs. pancreas T2\* values obtained on the dedicated liver MRI study (x-axis) ( $n = 127$ ;  $r = 0.27$ ; 95% CI 0.10–0.43;  $p = 0.0019$ ). Solid blue line is the line of best fit with the dotted red lines representing the 95% prediction limits for the best fit line.

quires dedicated images of both the liver and heart to quantify the iron contents in each organ.

Our study shows that it is possible to measure cardiac and liver T2\* on a single image sequence by taking advantage of the fact that the field of view for the cardiac T2\* sequence includes a portion of the liver because it needs to be extended inferiorly to avoid body wrap in the double oblique positioning for the cardiac measure. The significance of this finding is in terms of resource utilization, as this makes it possible to shorten the overall examination time and to limit the number of examinations performed and thus reduces healthcare costs. T2\* values for the liver obtained from the cardiac images are strongly and positively correlated with values obtained from dedicated liver images with a mean bias of only 0.5 ms. Notably there were only six pairs of exams that were outliers in terms of the difference in T2\* measurements. Four of the six outliers had mean T2\* > 20 ms and two had mean T2\* between 10 and 20 ms, values corresponding to normal/no iron overload and mild to moderate overload, respectively [16]. While the need for highly accurate T2\* values in the normal range is uncertain, if such accuracy were needed, either the  $\Delta TE$  or the number of echoes could be increased. Notably, in our study, no patients were incorrectly classified with abnormal T2\* measurements.

One limitation of the combined approach is that, due to the technical limitations of the myocardial T2\* acquisition and the minimum TE that could be achieved with older-generation MR hardware, livers with the lowest T2\* values and highest iron concentrations may be unable to be accurately measured due to rapid signal decay. This limitation applied to ten examinations (7% of

examinations meeting inclusion criteria) in four patients in our study cohort. This small subset of patients may still require dedicated images of the liver with a shorter minimum TE. Alternatively, current-generation MRI scanners with high gradient capacity that allow the first TE to be reduced or newer methods such as ultra-short TE (UTE)-based sequence, which allows for very short TE (~ 100 to 200  $\mu s$ ) between signal excitation and data acquisition, may help alleviate this limitation [17–21]. Despite this limitation, in patients with considerable iron overload and liver T2\* values < 5 ms, in whom measurements could still be made, there was moderate to strong correlation between liver T2\* values obtained on dedicated liver and cardiac MRI examinations with a mean bias of only 0.4 ms. Thus, with the exception of the small number of patients (7%) with the very high levels of liver iron that had to be excluded due to insufficient signal in the first TE of the cardiac T2\* study, a single examination covering both the heart and liver can allow measurement of both myocardial and liver T2\* with reasonable accuracy.

One other potential limitation of a combined cardiac and liver imaging approach is that if this method were to be implemented in practice, and only a single sequence was obtained, the entire liver would not be screened for focal lesions which can develop in patients with iron overload.

In addition to the liver, the pancreas and heart also accumulate circulating non-transferrin-bound iron (NTBI) [22–24]. As a result, the iron burdens in these organs should be correlated, although they may load at different rates. Recent works by Wood et al. in patients with thalassemia major and sickle cell disease support this hypothesis [23, 25]. In our study, pancreas T2\* correlated with liver T2\*, liver T2\* correlated with myocardium T2\*, and pancreas T2\* correlated with myocardium T2\*. Although these correlations were significant, they were not particularly strong, suggesting that a separate T2\* may need to be measured for each organ and using correlations from one organ may not be sufficient for diagnosis and quantification of other organs. Newer 3D mDixon-based techniques that automatically generate T2\* maps may allow accurate T2\* measurements in multiple organs [6, 17].

Our study has a few limitations: First, this was a retrospective study with available datasets limited to clinically indicated examinations that likely do not adequately encompass the full spectrum of diseases associated with iron deposition; indeed, most patients in our study had beta thalassemia or Diamond–Blackfan anemia. Second, our population was relatively small with few patients with the highest LIC; however, this is the first such study comparing liver T2\* measured on two separate studies of the same patient, acquired on the same scanner on the same day, and our results show that the T2\* of the liver is accurate and valid on these subjects

using either the cardiac study or the dedicated liver study. Furthermore, the liver T2\* measurements from dedicated liver MRI and cardiac MRI are very highly positively correlated with a very small number of outliers, indicating strong agreement.

## Conclusion

Liver T2\* measured from dedicated liver MR imaging and measured in the portion of the liver included in dedicated cardiac MR imaging are highly correlated, suggesting that both liver T2\* and cardiac T2\* can be calculated from a single MRI acquisition, reducing cost, MRI scanner time, and potentially the need for sedation in young patients. A relatively small number of patients with very high LIC (e.g., T2\* < 5 ms) may require a dedicated liver imaging study. Although T2\* correlations are significant between liver, pancreas, and heart, the correlation strength is weak suggesting T2\* values should be measured in each organ individually.

### Compliance with ethical standards

**Funding** No funding was received for this work.

**Conflict of interest** None.

**Ethical approval** All procedures performed in studies involving human participants were in accordance with the ethical standards of the institutional and/or national research committee and with the 1964 Helsinki declaration and its later amendments or comparable ethical standards.

**Informed consent** This was an IRB-approved HIPAA-compliant retrospective study and the need for informed consent was waived by the IRB.

## References

- Lieu PT, Heiskala M, Peterson PA, Yang Y (2001) The roles of iron in health and disease. *Mol Asp Med* 22(1–2):1–87
- Ware HM, Kwiatkowski JL (2013) Evaluation and treatment of transfusional iron overload in children. *Pediatr Clin N Am* 60(6):1393–1406
- Regev A, Berho M, Jeffers LJ, et al. (2002) Sampling error and intraobserver variation in liver biopsy in patients with chronic HCV infection. *Am J Gastroenterol* 97(10):2614–2618
- Towbin AJ, Serai SD, Podberesky DJ (2013) Magnetic resonance imaging of the pediatric liver: imaging of steatosis, iron deposition, and fibrosis. *Magn Reson Imaging Clinics N Am* 21(4):669–680
- Serai SD, Fleck RJ, Quinn CT, Zhang B, Podberesky DJ (2015) Retrospective comparison of gradient recalled echo R2\* and spin-echo R2 magnetic resonance analysis methods for estimating liver iron content in children and adolescents. *Pediatr Radiol* 45(11):1629–1634
- Serai SD, Smith EA, Trout AT, Dillman JR (2017) Agreement between manual relaxometry and semi-automated scanner-based multi-echo Dixon technique for measuring liver T2\* in a pediatric and young adult population. *Pediatr Radiol* 48:94–100
- Wood JC, Zhang P, Rienhoff H, Abi-Saab W, Neufeld EJ (2015) Liver MRI is more precise than liver biopsy for assessing total body iron balance: a comparison of MRI relaxometry with simulated liver biopsy results. *Magn Reson Imaging* 33(6):761–767
- Hankins JS, McCarville MB, Loeffler RB, et al. (2009) R2\* magnetic resonance imaging of the liver in patients with iron overload. *Blood* 113(20):4853–4855
- Sirlin CB, Reeder SB (2010) Magnetic resonance imaging quantification of liver iron. *Magn Reson Imaging Clin N Am* 18(3):359–481, ix
- Wood JC (2014) Use of magnetic resonance imaging to monitor iron overload. *Hematol Oncol Clin N Am* 28(4):747–764
- Wood JC, Enriquez C, Ghugre N, et al. (2005) MRI R2 and R2\* mapping accurately estimates hepatic iron concentration in transfusion-dependent thalassemia and sickle cell disease patients. *Blood* 106(4):1460–1465
- Pepe A, Positano V, Santarelli MF, et al. (2006) Multislice multi-echo T2\* cardiovascular magnetic resonance for detection of the heterogeneous distribution of myocardial iron overload. *JMRI* 23(5):662–668
- Positano V, Pepe A, Santarelli MF, et al. (2009) Multislice multi-echo T2\* cardiac magnetic resonance for the detection of heterogeneous myocardial iron distribution in thalassaemia patients. *NMR Biomed* 22(7):707–715
- Alustiza JM, Emparanza JI, Castiella A, et al. (2015) Measurement of liver iron concentration by MRI is reproducible. *Biomed Res Int* 2015:294024
- Brittenham GM, Cohen AR, McLaren CE, et al. (1993) Hepatic iron stores and plasma ferritin concentration in patients with sickle cell anemia and thalassemia major. *Am J Hematol* 42(1):81–85
- Anderson LJ, Westwood MA, Holden S, et al. (2004) Myocardial iron clearance during reversal of siderotic cardiomyopathy with intravenous desferrioxamine: a prospective study using T2\* cardiovascular magnetic resonance. *Br J Haematol* 127(3):348–355
- Serai SD, Dillman JR, Trout AT (2017) Proton density fat fraction measurements at 1.5- and 3-T hepatic MR imaging: same-day agreement among readers and across two imager manufacturers. *Radiology* 284:244–254
- Krafft AJ, Loeffler RB, Song R, et al. (2017) Quantitative ultra-short echo time imaging for assessment of massive iron overload at 1.5 and 3 Tesla. *Magn Reson Med* 78(5):1839–1851
- Doyle EK, Toy K, Valdez B, et al. (2017) Ultra-short echo time images quantify high liver iron. *Magn Reson Med* 79:1579–1585
- Roach DJ, Cremillieux Y, Fleck RJ, et al. (2016) Ultrashort echo-time magnetic resonance imaging is a sensitive method for the evaluation of early cystic fibrosis lung disease. *Ann Am Thorac Soc* 13:1923–1931
- Serai SD, Laor T, Dwek JR, Zbojniec AM, Carl M (2014) Feasibility of ultrashort TE (UTE) imaging of children at 1.5 T. *Pediatr Radiol* 44(1):103–108
- Azarkeivan A, Hashemieh M, Shirkavand A, Sheibani K (2016) Correlation between heart, liver and pancreas hemosiderosis measured by MRI T2\* among thalassemia major patients from Iran. *Arch Iran Med* 19(2):96–100
- Noetzi LJ, Papudesi J, Coates TD, Wood JC (2009) Pancreatic iron loading predicts cardiac iron loading in thalassemia major. *Blood* 114(19):4021–4026
- Papakonstantinou O, Alexopoulou E, Economopoulos N, et al. (2009) Assessment of iron distribution between liver, spleen, pancreas, bone marrow, and myocardium by means of R2 relaxometry with MRI in patients with beta-thalassemia major. *JMRI* 29(4):853–859
- Meloni A, Puliyl M, Pepe A, et al. (2014) Cardiac iron overload in sickle-cell disease. *Am J Hematol* 89(7):678–683